UDC 625.717

Air Force Education and Research Centre Zhukovsky and Gagarin Air Force Academy (Voronezh)
Ph.D. in Engineering, Assoc. Prof., Head of Dept. of Engineering and Airfield Maintenance A. N. Popov
Ph.D. student of Dept. of Engineering and Airfield Maintenance A. A. Khatuntsev
Russia, Voronezh, tel.: +7-919-246-70-03, e-mail: anton. hatun@yandex.ru

A. N. Popov, A. A. Khatuntsev

COMPUTING EXPERIMENTAL FACTOR MODEL OF THE MULTILAYERED AIRFIELD PAVEMENTS TAKING INTO ACCOUNT PHYSICAL NON-LINEARITY OF MATERIALS OF CONSTRUCTIVE LAYERS

Statement of the problem. For the definition of the characteristics of the interlaminar layer which are slowing down process of formation of reflected cracks in asphalt layers of strengthening of precast airfield pavements, carrying out of a series of the experiments which generalization of results will allow one to design an experimental factorial model is necessary.

Results. The results of computing experiments and the analysis of the mode of deformation of interlaminar layer interrupting a crack asphalt a layer of a reinforcement depending on design data and alternatives of the application of wheel loading are presented. Regression equations and nomogramm of the dependence of the stress arising on border of contact of interlaminar layer interrupting a crack and a precast airfield pavement in the field of a seam, on an elastic modulus, a thickness and a variant application of wheel loading are suggested.

Conclusions. The obtained regression model and nomogram constructed based on it helps determine the optimum characteristics of interlaminar layer interrupting a crack and can be used while designing layers of the strengthening of precast airfield pavement

Keywords: computing experiment, regression model, nomogram, airfield pavement.

Introduction

The analysis of ways of restoring the performance of composite airfirled pavements of airfield smooth plates (PAG) by enhancing the effort using asphalt concrete reinforcement [1] suggests that a crack-intercepting layer between the plates and the asphalt concrete reinforcement layer will reduce reflected cracks emerging in the latter.

In order to validate the hypothesis, a series of computing experiments was carried out on software using a theoretical model with their results enabling the design of an experimental factor model. This method is preferred due to small financial and time costs for providing credible re-

sults. Besides, it was considered that software for implementing the finite element method has advanced significantly.

Unlike theoretical ones, experimental factor models do not make use of the physical laws describing what is happening in objects but are some formal dependencies of internal and external parameters of objects being constructed.

The experiment can be divided into five stages [2]: stating the problem, choosing optimal values and varying factors, choosing the experiment plan and identifying the research scope, performing the experiments according to the plan, getting findings and conclusions based on the analysis of the suggested model.

1. Stating the problem, choosing the optimal values and varying factors. The objective of the experiment is to study the impact of the characteristics of crack-intercepting layer on the stress strain of the asphalt concrete of a composite airfield pavement using smooth plates (PAG) under a mechanical load of a four-axle support of an aircraft. The impact of the elasticity modulus $E_{\text{ТПП}}$ as well as the thickness $t_{\text{ТПП}}$ on the tensile stress σ_x in the crack-intercepting layer over the joint of the airfield pavement made of smooth plates (PAG) was assessed.

The characteristics of crack-intercepting layers of a multilayered airfield pavement were modelled using a regression analysis by means of the least square method.

The experimental factor model was designed according to the principal scheme as shown in Fig. 1 based on the computing active experiments in *COMSOL Multiphysics* using the theoretical model. The aim was to identify the optimal criteria describing the efficiency and quality of the reinforcement structure of a composite airfield pavement made of smooth plates (PAG).

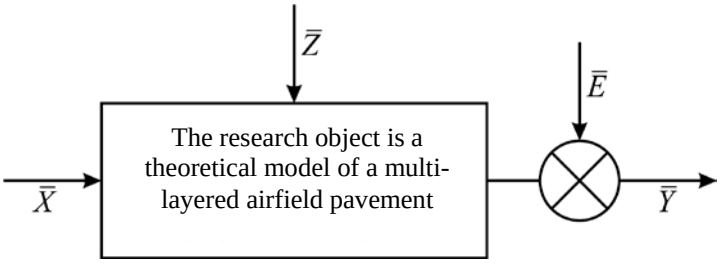

Fig. 1. Principal scheme of the experimental factor model [2]: $\bar{X}$ are controlled and manipulated factors; $\bar{Z}$ are controlled and non-manipulated factors; $\bar{E}$ are interferences; $\bar{Y}$ is a response

The research object was chosen to be a theoretical mathematical model of a multilayered airfield pavement designed using the mathematical hypotheses of the fluidity and accounting for physical non-linearity of the materials of the construction layers [3].

The number of controlled and manipulated factors $\overline{X}$, impacting the research object is restrained by these two: x_1 is the elasticity modulus $E_{\text{ТПП}}$, MPa; x_2 is the thickness $t_{\text{ТПП}}$, mm.

Controlled and manipulated factors $\overline{Z}$, typical of natural experiments were missing as computing active software experiments involving the theoretical model were being performed [2].

Interferences $\overline{E}$ are due to the size of the finite elements that are used for approximating the geometry of the model. Since the value in question remains identical in the range of one finite element, thus the smaller is the size of a finite element, the less flawed is the study. The effect of interferences $\overline{E}$ is accounted for by means of the regression analysis.

The output property of the model (response) $\overline{Y}$ is the resistance σ_x on the foot of the crack-intercepting layer in the plane crossing the joint of the composite airfield pavement.

The calculation loading was that of the major four-wheel support VS n_k = 4 with the internal air pressure in the wheel pneumatics p_a = 1 MPa, the distance between the adjoining wheels is 0.7 m, between the rows of wheels is 1.3 m. The dynamic coefficient k_d and unloading γ_f accounting for the motion on the airfield pavement were chosen to be less favourable for the pavement of this type k_d = 1.2, γ_f = 1, which corresponds with Group A of airfield pavement areas. The loading onto the wheel support F_n was accepted to be maximum permissible for composite airfield pavements from typical slabs PAG–14 — F_n = 400 kN. The calculation scheme of the major support of the airfield pavement is shown in Fig. 2.

The loading F_a of each wheel onto the major support evenly distributed along the imprint was

$$F_a = \frac{F_d}{\pi R_e^2} = 1 \text{ MN/m}^2, \quad (1)$$

where F_d is the calculation loading onto the wheel:

$$F_d = \frac{F_n}{n_k} k_d \gamma_f = 120 \text{ kN};$$

R_e is the radius of the circle as large as the area of the imprint of the wheel pneumatics:

$$R_e = \sqrt{\frac{F_d}{\pi p_a}} = 0.195 \text{ m}.$$

The calculation options in the computing experiment were loads as shown in Fig. 3 for which there were responses $\tilde{Y}_1$, $\tilde{Y}_2$, $\tilde{Y}_3$.

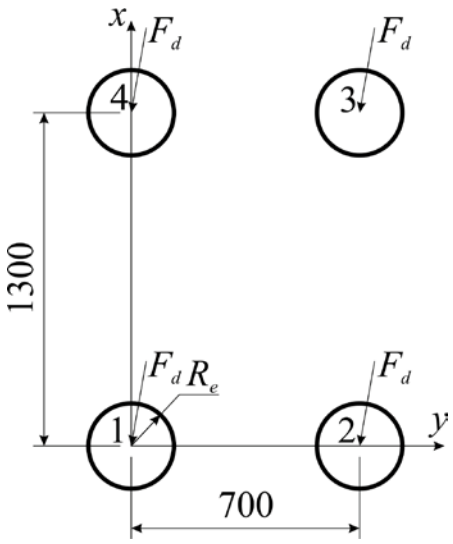

Fig. 2. Calculation scheme of a four-wheel support VS

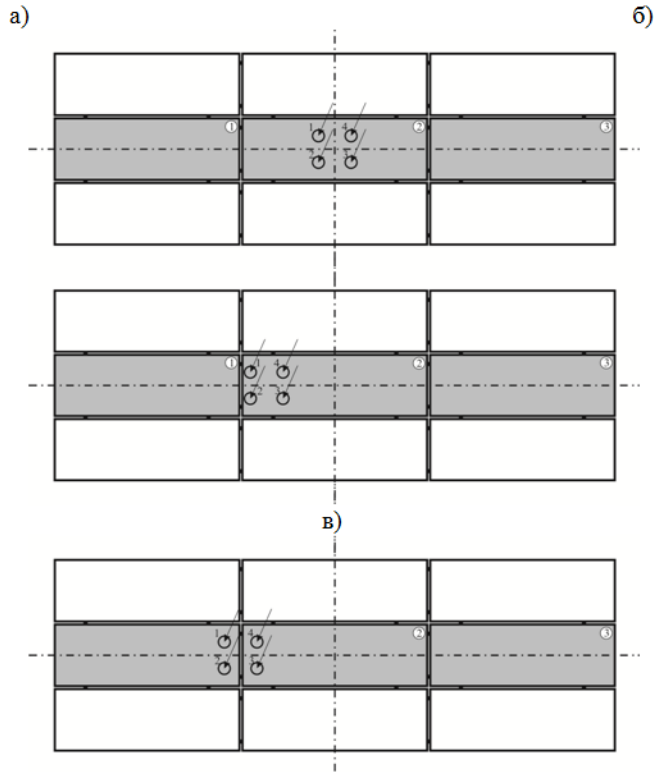

Fig. 3. Load application options of the four-wheel support VS:
a) central loading of the slab (option 1);
b) edge loading of the slab (option 2);
c) edge loading of the adjoining slabs (option 3)

2. Planning the experiment, identifying the research scope, processing the results and statistical analysis of the resulting model. In order to obtain a secod order regression model, a central composite planning set forth by G. E. P. Box and K. B. Wilson [4]. Geometric representation of the planning area is in Fig. 4 and ratability central composite second-order uniform plan is in Table.

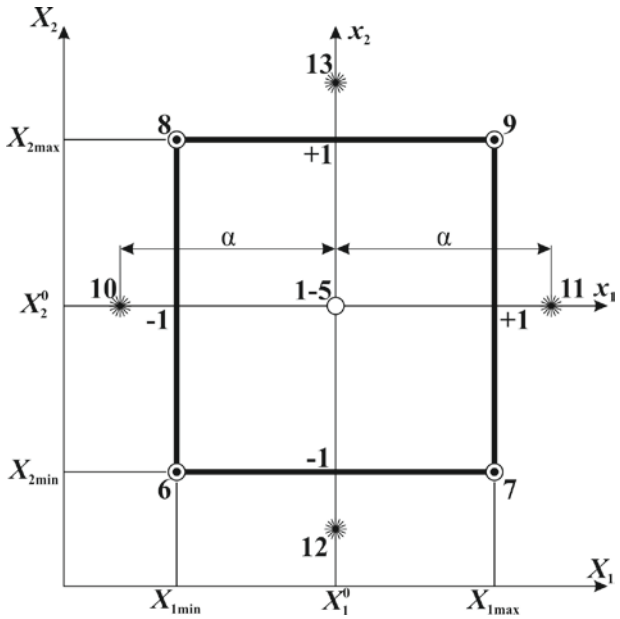

Fig. 4. Geometric representation in the ratability composite uniform plan

As a result of the experiment using the ratability central composite uniform plan of the second order the following responses presented as vectors were obtained:

$$\tilde{Y}_1 = (0.266;\ 0.266;\ 0.266;\ 0.266;\ 0.266;\ -0.153;\ 0.139;\ 0.256;\ 0.293;\ 0.209;\ 0.281;\ 0.213;\ 0.148)^T,$$
$$\tilde{Y}_2 = (3.153;\ 3.153;\ 3.153;\ 3.153;\ 3.153;\ 3.442;\ 4.843;\ 2.528;\ 3.354;\ 2.165;\ 3.530;\ 4.405;\ 3.105)^T,$$
$$\tilde{Y}_3 = (2.209;\ 2.209;\ 2.209;\ 2.209;\ 2.209;\ 2.527;\ 3.000;\ 1.868;\ 1.963;\ 1.935;\ 2.270;\ 3.428;\ 3.358)^T,$$
$$\hat{y}_1 = 0.266 + 0.054x_1 + 0.059x_2 - 0.03x_1^2 - 0.062x_2^2 - 0.064x_1x_2. \quad (2)$$

As a result, for each option of the wheel load application, there is a unique regression model:

$$\hat{y}_1 = 0.266 + 0.054x_1 + 0.059x_2 - 0.03x_1^2 - 0.062x_2^2 - 0.064x_1x_2, \quad (3)$$

$$\hat{y}_2 = 3.153 + 0.52x_1 - 0.53x_2 - 0.094x_1^2 + 0.359x_2^2 - 0.144x_1x_2, \quad (4)$$

$$\hat{y}_3 = 2.209 + 0.13x_1 - 0.224x_2 - 0.156x_1^2 + 0.488x_2^2 - 0.094x_1x_2. \quad (5)$$

The quality of prediction provided by the obtained regression models was estimated using the Fisher criterion F and coefficient of determination R^2 [2].

In all three cases $F > F_{кр}$, $R^2 > 0.75$ and the regression models are thus sufficient and operational.

Since in second-order regression models the coefficients are not normally estimated [2], the model was not made more simple and the complete square polynomial was used.

Table

Ratability central composite uniform-plan of the second order

Factors and function of the response		$E_{ТПП}$	$t_{ТПП}$	$E_{ТПП}^2$	$t_{ТПП}^2$	$E_{ТПП} \cdot t_{ТПП}$	σ_x
Code	x_0	x_1	x_2	x_1^2	x_2^2	x_1x_2	$\tilde{Y}$
Value units		10^3 MPa	mm				MPa
Main level (0)		8.8	190				
Variation range (I)		3.7	78				
Upper level (+1)		12.5	268				
Lower level (–1)		5.1	112				

End of Table

Factors and function of the response			$E_{ТПП}$	$t_{ТПП}$	$E_{ТПП}^2$	$t_{ТПП}^2$	$E_{ТПП} \cdot t_{ТПП}$	σ_x
Star point (+α)			14	300				
Star point (–α)			3.6	80				
(1)	(2)	(3)	(4)	(5)	(6)	(7)	(8)	(9)
Central experiments	1	+1	0	0	0	0	0	y_1
	2	+1	0	0	0	0	0	y_2
	3	+1	0	0	0	0	0	y_3
	4	+1	0	0	0	0	0	y_4
	5	+1	0	0	0	0	0	y_5
Full factorial experiment 2^2	6	+1	–1	–1	+1	+1	+1	y_6
	7	+1	+1	–1	+1	+1	–1	y_7
	8	+1	–1	+1	+1	+1	–1	y_8
	9	+1	+1	+1	+1	+1	+1	y_9
Star points	10	+1	–1.414	0	+1.999	0	0	y_{10}
	11	+1	+1.414	0	+1.999	0	0	y_{11}
	12	+1	0	–1.414	0	+1.999	0	y_{12}
	13	+1	0	+1.414	0	+1.999	0	y_{13}

3. Analysis of the results of numerical modelling. The analysis of total deformations *S* of a multilayered airfield pavement showed that the boundary of the deflection bowl *D* is significantly larger that the imprint of the load applied and ranges from 15 to 18 m depending on the factor values. Similar behaviour of the structure indicates the significance of distribution properties of the base in describing deformation of the airfield pavement. A variant of load application was found to have no significant impact on total deformations of the pavement *S*. The maximum difference in *S* from Fig. 5 is observed in the experiment 6 (2.28—2.59 mm), experiment 7 (2.03—2.36 mm) and experiment 12 (2.20—2.60 mm), in the remaining experiments it is no more than 0.17 mm.

An increase in the elasticity modulus $E_{ТПП}$ and (or) thickness $t_{ТПП}$ causes a decrease in total deformations of the pavement *S* according to the non-linear law. The graph in Fig. 6 sug-

gests that an increase in the elasticity modulus $E_{\text{ТПП}}$ from $3.6 \cdot 10^3$ MPa to $14 \cdot 10^3$ MPa at $t_{\text{ТПП}}$ = 190 mm and edge loading causes a decrease in total deformations of the pavement S from 1.90 to 1.65 mm. At the same time, an increase in the thickness of the sublayer $t_{\text{ТПП}}$ from 80 to 300 mm at $E_{\text{ТПП}} = 8.8 \cdot 10^3$ MPa and edge loading is accompanied by a decrease in total deformations of the pavement S from 2.31 to 1.56 mm (Fig. 7).

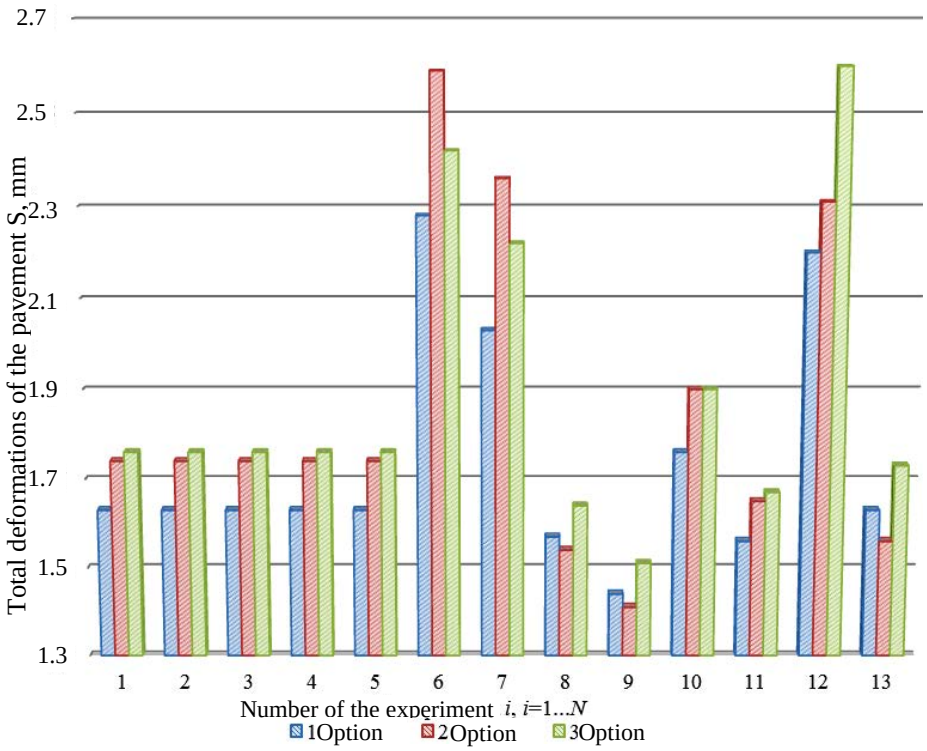

Fig. 5. Histogram of change in total deformations S depending on the load application pattern and varying factors in the experiment i, $i = 1…N$

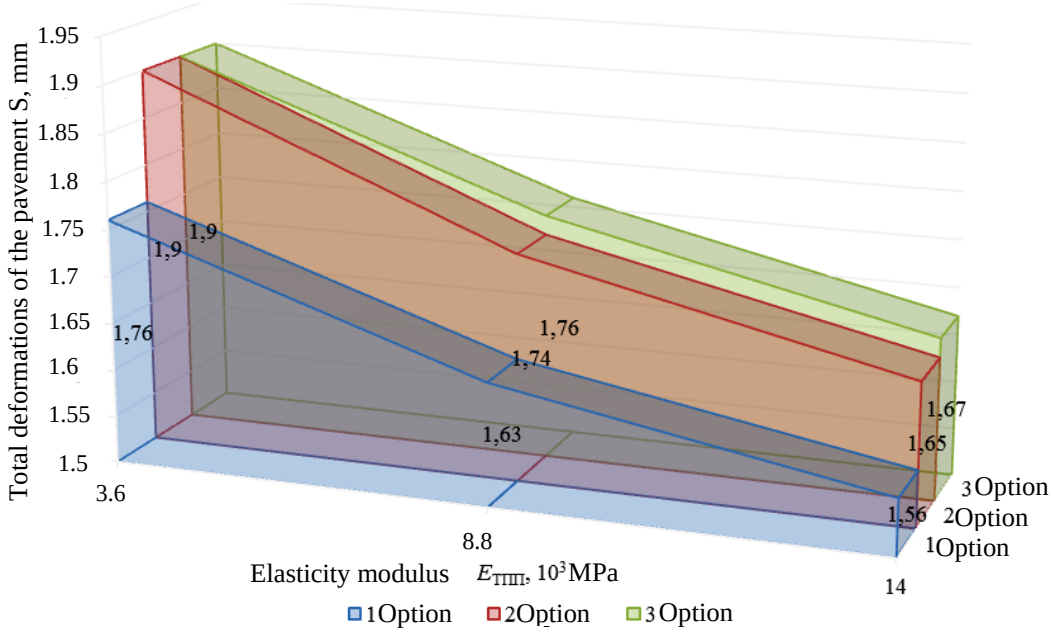

Fig. 6. Graph of the dependence of total deformations S on the elasticity modulus $E_{\text{ТПП}}$ at $t_{\text{ТПП}}$ = 190 mm

A subsequent increase in the loading up to P_C causes plastic deformations to accumulate and the dependence between the loading and heaving of the pavement becomes non-linear (section BC), i.e. the pavement is in the elastic plastic stage. As the airfield pavement is unloaded, the diagram coincides with the straight line CD almost parallel to the original area of the diagram AB. Another loading generates solely elastic deformations (according to the straight line CD) until the loading reaches P_C again, followed by the accumulation of extra plastic deformations.

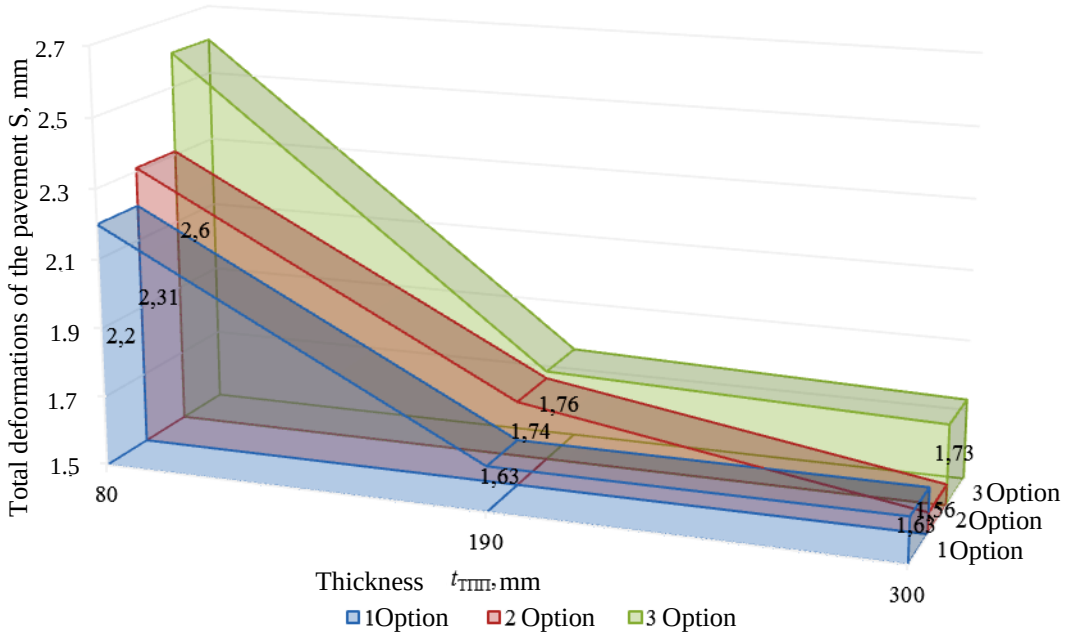

Fig. 7. Graph of the dependence of total deformations S on the thickness $t_{ТПП}$ at $E_{ТПП} = 8.8 \cdot 10^3$ MPa

As a result of mechanical loading in all the construction layers of the airfield pavement there are areas of plastic deformations. There are residual deformations induced by wheel load in the artificial pavement and in the base along the perimeter of PAG slabs responding to and redistributing the loading onto the lower layers.

The cause of plastic deformations emerging in the artificial pavement is the stress tensor deviator, in construction layers of artificial and natural bases it is the deviation and hydrostatic component of the stress strain.

Isofields of stress tensor deviator are shaped identically with those of normal stresses but are less. This makes sense considering the stress deviator D_σ is [5]:

$$D_\sigma = T_\sigma - T_{\sigma_0} = \begin{vmatrix} \sigma_x - \sigma_0 & \tau_{xy} & \tau_{xz} \\ \tau_{xy} & \sigma_y - \sigma_0 & \tau_{yz} \\ \tau_{xz} & \tau_{yz} & \sigma_z - \sigma_0 \end{vmatrix}, \quad (6)$$

where σ_0 is an octahedral normal stress:

$$\sigma_0 = \frac{1}{3}\left(\sigma_x + \sigma_y + \sigma_z\right).$$

It is obvious that the difference between the isofields is the octahedral normal stress and stress deviator elements except diagonal ones are identical with those of the stress tensor.

The analysis of the deformations of the airfield (Fig. 8) indicates that the dependence between the loading and heaving is in the section AB to the loading P_B when the airfield pavement is in the elastic stage and Hooke's law holds true.

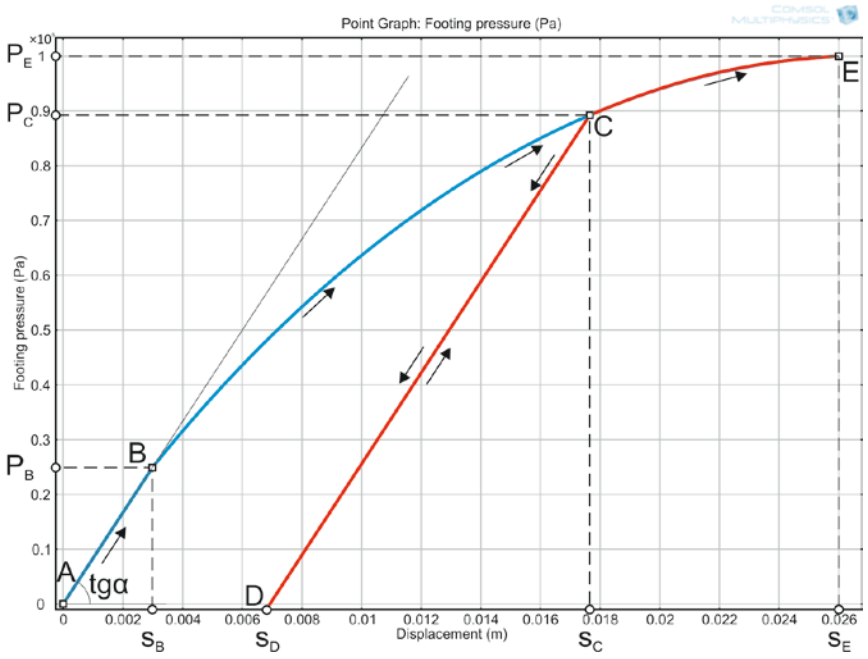

Fig. 8. Graph of the dependence of the heaving of the pavement on the loading at $E_{\text{ТПП}} = 8.8 \cdot 10^3$ MPa, $t_{\text{ТПП}} = 80$ mm

The distributions of normal stresses σ_x in crack-intercepting layers along the wheel support given in Fig. 9 enable a study of change of stresses depending on which load application option there is on a section restrained by temperature joints along the longitudinal axis X which is $t_{\text{ТПП}}/2$ deep.

Central loading causes maximum stresses σ_x to emerge where the wheel load is applied and in temperature joints (Fig. 9a), over the transverse joints are close to zero. There is symmetry in relation to the centre of the wheel load.

In edge loading and that of adjoining slabs (Fig. 9b, c) the distribution of normal stresses σ_x is shaped identically:

— a dramatic change in stresses σ_x over the transverse joint where the load is applied and in the temperature joint of the slab 1;

— almost zero σ_x over the temperature and transverse joints removed from the application of the wheel load.

The distribution of normal stresses σ_x in crack-intercepting layers thus indicates their concentration over the transverse joints of the composite airfield pavement of PAG slabs where the load is applied as well as in edges of the temperature joints. Most likely to have reflected cracks are areas of crack-intercepting layers over the transverse joints of the composite airfield of PAG slabs. The maximum tensile stresses σ_x in crack-intercepting layers over the transverse joints of the airfield pavement is during the edge loading and is at its minimum under central loading.

a)

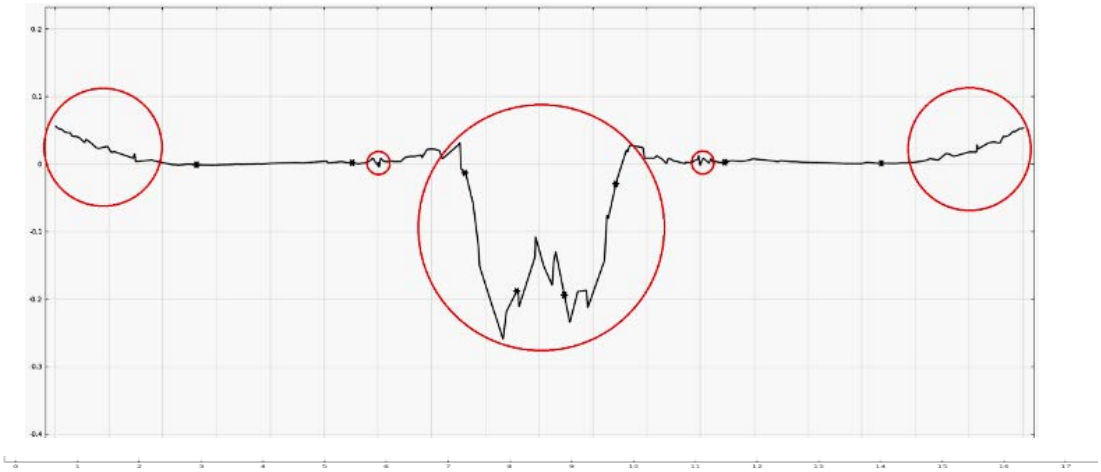

b)

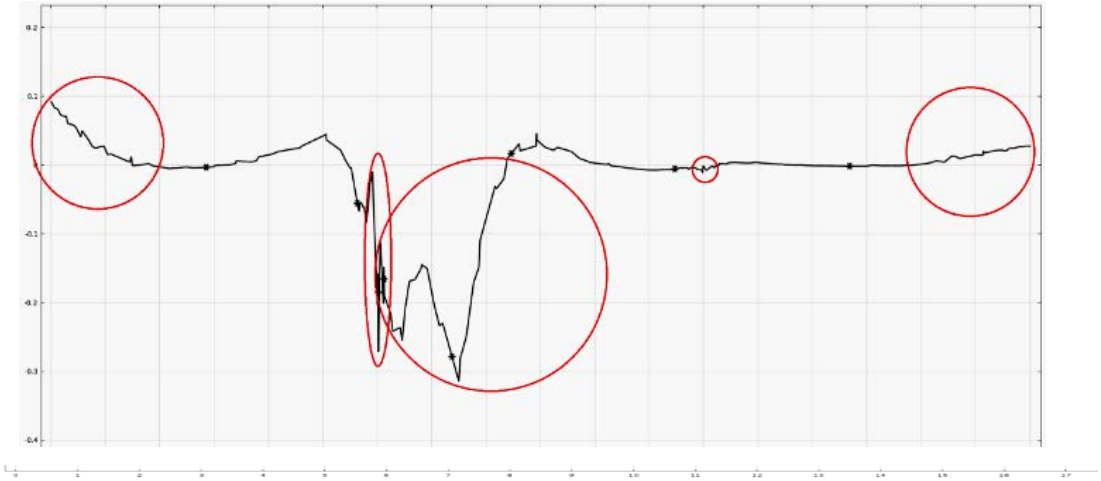

Fig. 9. Stress distribution σ_x in the section along the axis X_1
at $E_{TIIII} = 8.8 \cdot 10^3$ MPa, $t_{TIIII} = 190$ mm:
a) central loading;
b) edge loading

c)

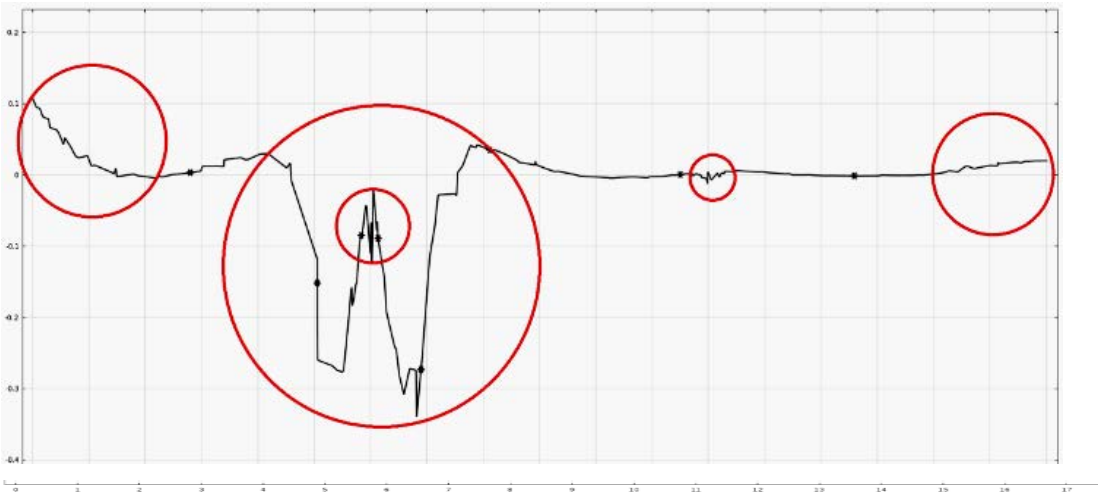

Fig. 9. Stress distribution σ_x in the section along the axis X_1 at E_{TTTT} = 8.8·10^3 MPa, t_{TTTT} = 190 mm:
c) loading of the adjoining slabs

An increase in the elasticity modulus $E_{\text{ТПП}}$ at fixed thickness $t_{\text{ТПП}}$ causes an increase in the normal stresses σ_x non-linearly (Fig. 10).

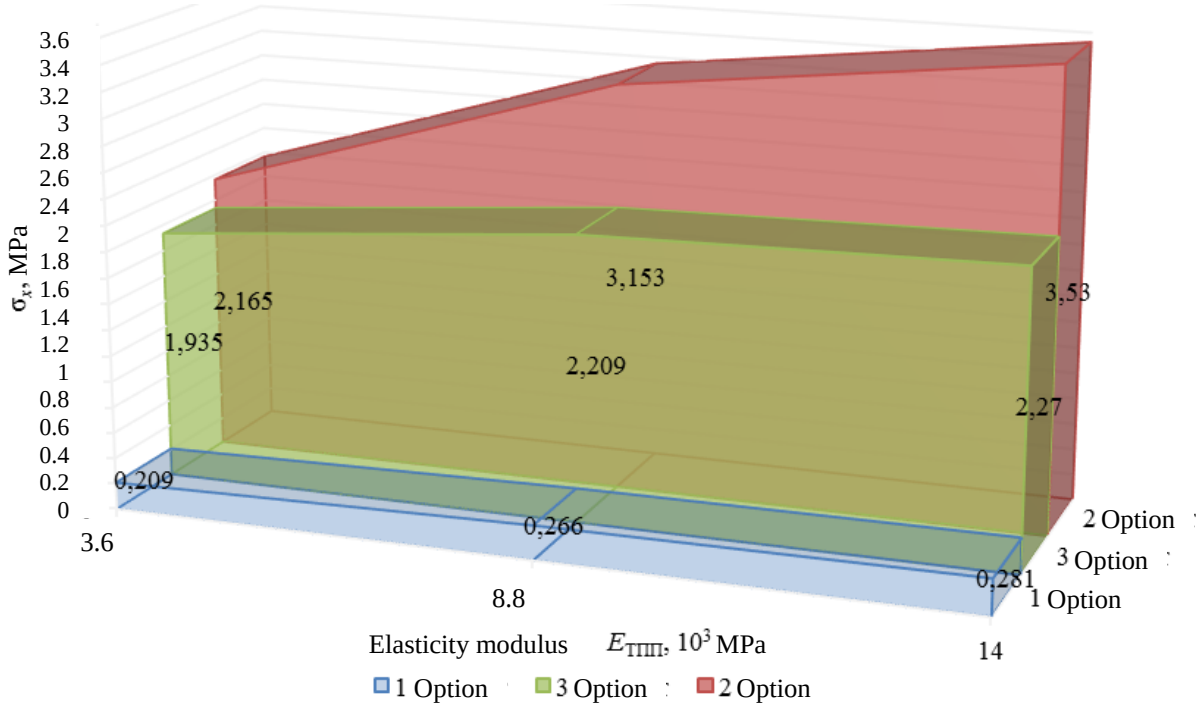

Fig. 10. Graph of the dependence of the stresses σ_x on the elasticity modulus $E_{\text{ТПП}}$ at $t_{\text{ТПП}}$ = 190 mm

The behaviour of the curved line as the thickness $t_{\text{ТПП}}$ increases and fixed elasticity modulus $E_{\text{ТПП}}$ (Fig. 11) depends on the load application option.

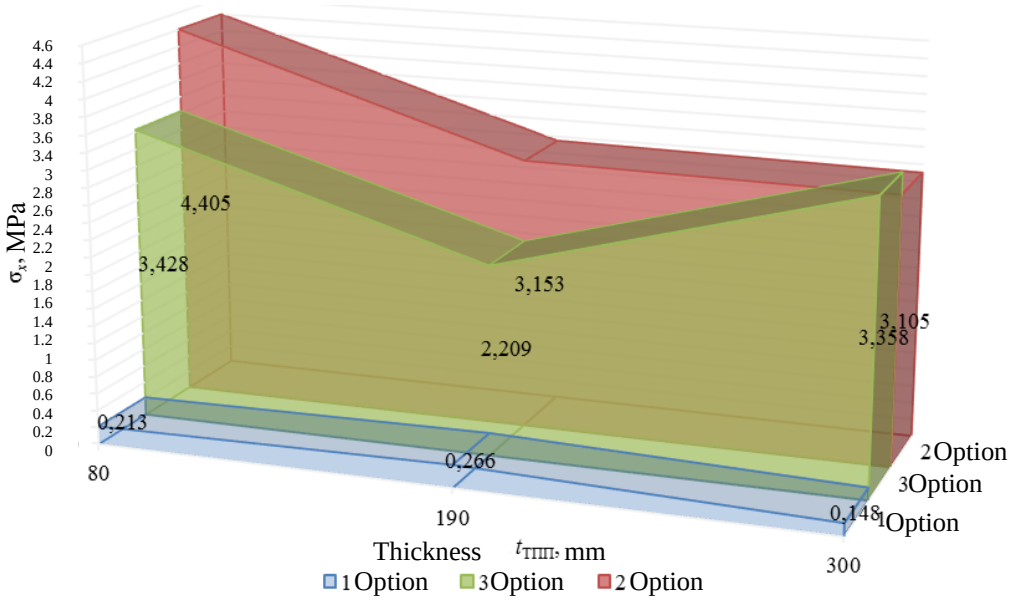

Fig. 11. Graph of the dependence of the stresses σ_x on the thickness $t_{ТПП}$ at $E_{ТПП} = 8.8 \cdot 10^3$ MPa

Under edge loading causing the largest stresses in the crack-intercepting layers over the transverse joint of the composite pavement, an increase in the thickness $t_{ТПП}$ from 80 to 190 mm causes a dramatic decrease in the stresses σ_x. Subsequent increase in the thickness causes no significant decrease in the stresses. The diagrams of normal stresses σ_x (Fig. 12) along the vertical axis over the joint of the composite airfield pavement along the wheel support indicated that an increase in the elasticity modulus $E_{ТПП}$ at a fixed thickness $t_{ТПП}$ besides an increase in the tensile stresses is accompanied by an increase in the tension region.

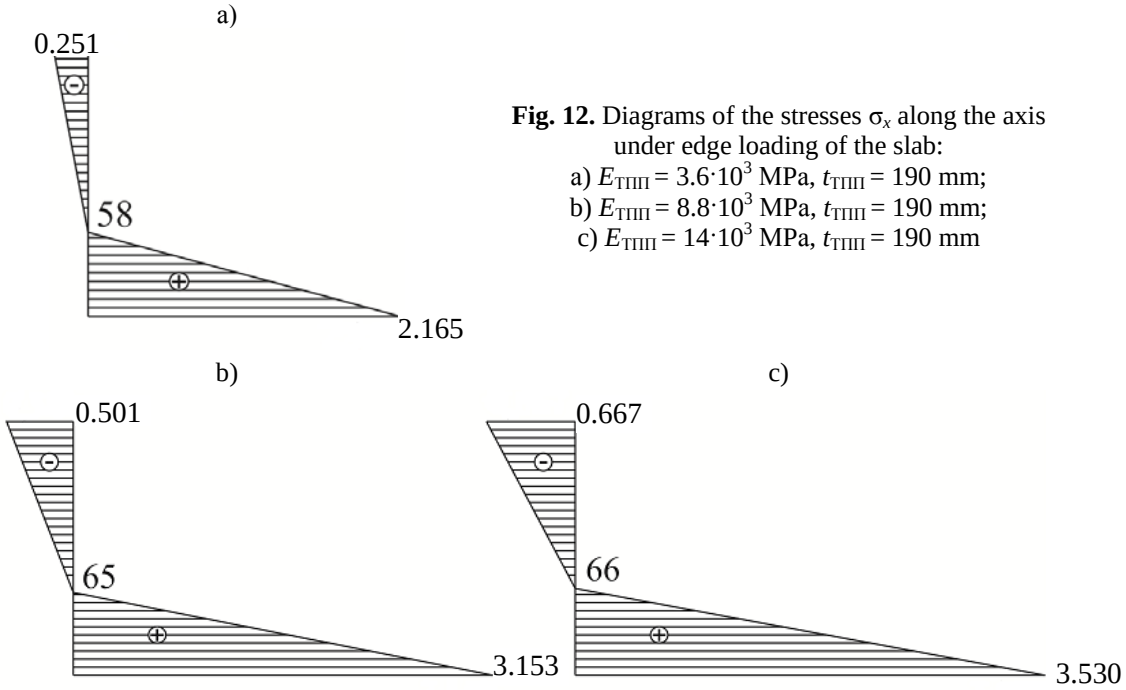

Fig. 12. Diagrams of the stresses σ_x along the axis under edge loading of the slab:
a) $E_{ТПП} = 3.6 \cdot 10^3$ MPa, $t_{ТПП} = 190$ mm;
b) $E_{ТПП} = 8.8 \cdot 10^3$ MPa, $t_{ТПП} = 190$ mm;
c) $E_{ТПП} = 14 \cdot 10^3$ MPa, $t_{ТПП} = 190$ mm

The calculation model was the second regression model (4) describing change in the stresses σ_x at the foot of the crack-intercepting layer in the plane crossing the joint of the composite airfield pavement under edge loading.

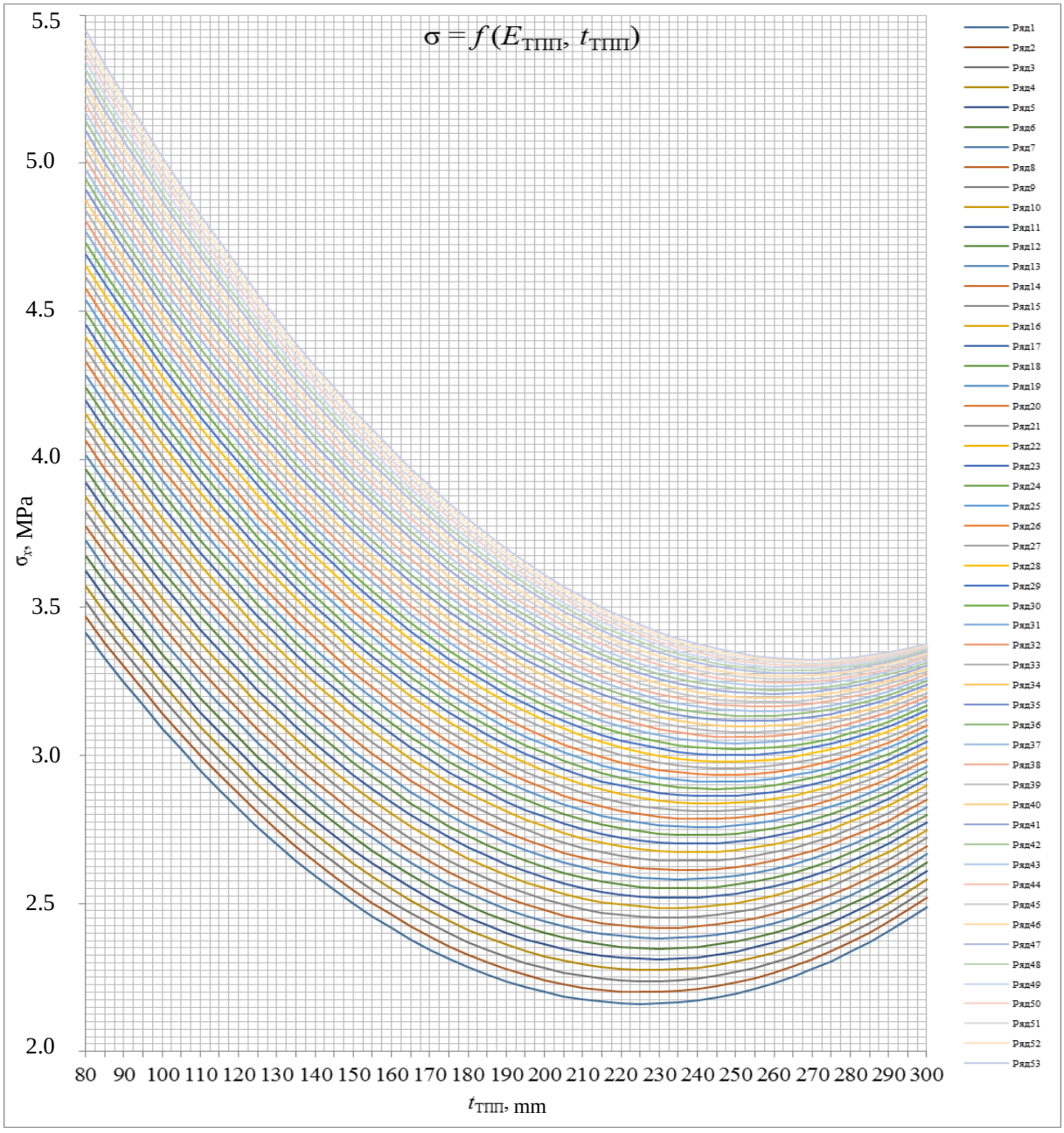

Fig. 13. Nomogram for identifying the thickness of the crack-intercepting layer using the elasticity modulus $E_{ТПП}$ and ultimate stresses σ_x in the tension region of the crack-intercepting layer

Considering the connection between the standard thicknesses and elasticity modulus of the crack-intercepting layers and their actual values:

$$x_1 = \frac{E_{ТПП} - 8.8}{3.7},\ x_2 = \frac{t_{ТПП} - 190}{78}, \qquad (7)$$

we have a dependence

$$\sigma_x = 3.97144 + 0.35619E_{\text{ТПП}} - 0.024827t_{\text{ТПП}} - \\ -0.006866E_{\text{ТПП}}^2 + 0.000059t_{\text{ТПП}}^2 - 0.000499E_{\text{ТПП}}t_{\text{ТПП}}. \quad (8)$$

Based on the dependence (8), there is a nomogram given in Fig. 13 and allowing one to identify the thickness of the crack-intercepting layer of an asphalt concrete reinforcement structure using the elasticity modulus $E_{\text{ТПП}}$ and ultimate stresses σ_x in the tension region of the crack-intercepting layer.

Conclusions

1. The regression models have been obtained describing change in the stresses of the crack-intercepting layer caused by the thickness and elasticity modulus of the crack-intercepting layer material for all the three load application options.

2. Based on the regression model for edge loading when the stresses are maximum, the nomogram was designed to identify the thickness of the crack-intercepting layer of an asphalt concrete reinforcement structure using the elasticity modulus $E_{\text{ТПП}}$ and ultimate stresses σ_x in the tension region of the crack-intercepting layer.

References

1. Khatuncev A. A., Popov A. N., Masalykin A. N. *Obosnovanie konstrukcii usileniya sbornyx ae'rodromnyx pokrytij iz plit PAG sloyami asfal'tobetona* [The rationale for strengthening structure of prefabricated airfield pavement of slabs PAG layers of asphalt concrete]. Moscow, 2013. 22 p. Dep. v CSIF MO RF 20.12.12, № V7422.

2. Tarasik V. P. *Matematicheskoe modelirovanie texnicheskix sistem.* 2-e izd., pererab. i dop. [Mathematical modeling of technical systems: textbook for universities. 2nd ed., revised and enlarged]. Minsk, Dizajn PRO Publ., 2004. 640 p.

3. Khatuncev A. A., Popov A. N., Volkov V. V. Uprugoplasticheskaya model' deformacii ae'rodromnogo pokrytiya po kriteriyu prochnosti Drukera — Pragera [The elastoplastic deformation model airfield pavements by the strength criterion of Drucker—Prager]. *Vestnik BGTU im. V. G. Shuxova*, 2013, no. 6, pp. 52—56.

4. Khartman K., Leckij E'. K., Shefer V. [i dr.] *Planirovanie e'ksperimenta v issledovanii texnologicheskix processov* [Experimental design in the study of technological processes]. Moscow, Mir Publ., 1977. 552 p.

5. Fadeev A. B. *Metod konechnyx e'lementov v geomexanike* [Finite element method in geomechanics]. M., Nedra Publ., 1987. 221 p.